Ecological Modelling 267 (2013) 127–137

Contents lists available at ScienceDirect

Ecological Modelling

journal homepage: www.elsevier.com/locate/ecolmodel

Incorporation of diet information derived from Bayesian stable isotope mixing models into mass-balanced marine ecosystem models: A case study from the Marennes-Oléron Estuary, France

Stephen R. Pacella[a,b,*], Benoit Lebreton[c], Pierre Richard[c], Donald Phillips[b], Theodore H. DeWitt[b], Nathalie Niquil[c]

[a] College of Earth, Ocean, and Atmospheric Sciences, Oregon State University, 104 Wilkinson Hall, Corvallis, OR 97331, USA
[b] Western Ecology Division, Office of Research and Development, National Health and Environmental Effects Research Laboratory, United States Environmental Protection Agency, 200 SW 35th Street, Corvallis, OR 97333, USA
[c] Université de la Rochelle-CNRS, UMR 6250, Littoral Environnement et Sociétés (LIENSs), 2 rue Olympe de Gouges, F-17000 La Rochelle, France

ARTICLE INFO

Article history:
Received 15 March 2013
Received in revised form 19 July 2013
Accepted 20 July 2013

Keywords:
Ecological model
Stable isotope
Inverse analysis
Food web
Seagrass

ABSTRACT

We investigated the use of output from Bayesian stable isotope mixing models as constraints for a linear inverse food web model of a temperate intertidal seagrass system in the Marennes-Oléron Bay, France. Linear inverse modeling (LIM) is a technique that estimates a complete network of flows in an underdetermined system using a combination of site-specific data and relevant literature data. This estimation of complete flow networks of food webs in marine ecosystems is becoming more recognized for its utility in understanding ecosystem functioning. However, diets and consumption rates of organisms are often difficult or impossible to accurately and reliably measure in the field, resulting in a large amount of uncertainty in the magnitude of consumption flows and resource partitioning in ecosystems. In order to address this issue, this study utilized stable isotope data to help aid in estimating these unknown flows. $\delta^{13}C$ and $\delta^{15}N$ isotope data of consumers and producers in the Marennes-Oléron seagrass system was used in Bayesian mixing models. The output of these mixing models was then translated as inequality constraints (minimum and maximum of relative diet contributions) into an inverse analysis model of the seagrass ecosystem. The objective of this study was to investigate how the addition of diet information gained from the stable isotope mixing models would help constrain a linear inverse food web model. In order to investigate this, two inverse food web models were built to track the flow of carbon through the seagrass food web on an annual basis, with units of mgC m^{-2} d^{-1}. The first model (Traditional LIM) included all available data, with the exception of the diet constraints formed from the stable isotope mixing models. The second model (Isotope LIM) was identical to the Traditional LIM, but included the Bayesian mixing model diet constraints. Both models were identical in structure, and intended to model the same Marennes-Oléron intertidal seagrass bed. Each model consisted of 27 compartments (24 living and 3 detrital) and 175 flows. Comparisons between the outputs of the models showed the addition of the Bayesian mixing model-derived isotopic diet constraints further constrained the solution range of all food web flows on average by 26%. Flows that were directly affected by an isotopic diet constraint were 45% further constrained on average. These results showed that incorporation of the isotope information resulted in a more constrained food web model, and demonstrated the benefit of utilizing multi-tracer stable isotope information in ecosystem models.

Published by Elsevier B.V.

1. Introduction

Current ecological questions are often complex in nature, requiring a holistic perspective in order to adequately address the multitude of variables and relationships. There is thus an ever-increasing pressure on ecologists to address these questions at the ecosystem scale. Quantitative food web models, representing partial or whole ecosystem flux networks, are a promising methodology to address ecological questions (Finn and Leschine, 1980; Christian et al., 2009; Leslie and McLeod, 2007). These models are able to simultaneously explore effects of environmental changes on ecosystem structure and function, as well as emergent properties such as system dependencies, recycling, and efficiencies (Niquil et al., 2012). Banašek-Richter et al. (2004) showed that ecosystem

* Corresponding author at: College of Earth, Ocean, and Atmospheric Sciences, Oregon State University, 104 Wilkinson Hall, Corvallis, OR 97331, USA.
Tel.: +1 412 952 2568.
E-mail address: spacella@coas.oregonstate.edu (S.R. Pacella).

0304-3800/$ – see front matter. Published by Elsevier B.V.
http://dx.doi.org/10.1016/j.ecolmodel.2013.07.018

descriptors based on quantified systems models are more accurate than their qualitative counterparts. Estimation of complete flux networks of food webs in marine ecosystems is recognized for its utility to understand ecosystem functioning (Niquil et al., 2012). However, many components of ecosystem models are understood conceptually, but difficult or impossible to measure in the field, and therefore must be estimated (Niquil et al., 1998; van Oevelen et al., 2010; Vezina and Platt, 1988).

Inverse analysis is a powerful quantitative modeling method for estimating unmeasured components in ecosystem structures and has been widely used for this reason in food web modeling (Breed et al., 2004; Daniels et al., 2006; Degré et al., 2006; Donali et al., 1999; Eldridge et al., 2005; Eldridge and Jackson, 1993; Grami et al., 2008, 2011; Jackson and Eldridge, 1992; Kones et al., 2009; Leguerrier et al., 2003, 2007; Niquil et al., 1998, 2006). It has become commonly referred to as linear inverse modeling (LIM). Similarly to ECOPATH with ECOSIM (Christensen and Pauly, 1992; Pauly, 2000; Walters et al., 1997), LIM produces a static, mass-balanced, temporally integrated snapshot of the complete food web. Recent methodological advances have resulted in moving from models being solved with a single objective function (frequently a minimization function, (Vezina and Platt, 1988), to utilizing stochastic Markov Chain Monte Carlo methods to produce probability distributions of model results (LIM-MCMC) (Kones et al., 2006, 2009; Van den Meersche et al., 2009; van Oevelen et al., 2010). This technique avoids underestimates in both the size and complexity of the modeled food web as a result of the parsimony principle (Johnson et al., 2009; Kones et al., 2006). A more thorough review on the subject is covered by Niquil et al. (2012). Few applied studies have made use of recent methodological advances in this field, despite the relevance to informing conservation and environmental management decisions (Christian et al., 2009).

Stable isotopes are commonly used to study trophodynamics in ecosystems. Stable isotope analyses allow determination of food sources actually assimilated in the tissues of consumers over time, properly reflecting their trophodynamics depending on food source availability. Consumption rates are often difficult or impossible to accurately measure in the field, especially for smaller organisms, resulting in a large uncertainty in the magnitude of consumption flows and trophic resource partitioning in ecosystem models. Stable isotope data can be utilized to estimate these unmeasured flows (Navarro et al., 2011; van Oevelen et al., 2010). While the use of stable isotopes in diet studies has become standard practice (Moore and Semmens, 2008; Post, 2002), the integration of stable isotope data with whole food web network models has not been utilized frequently (Baeta et al., 2011; Navarro et al., 2011). The merits of this technique have been discussed recently in the literature (Navarro et al., 2011; van Oevelen et al., 2010).

Until now, only one stable isotopic marker ($\delta^{13}C$ or $\delta^{15}N$) at a time has been incorporated into inverse analysis models (Eldridge et al., 2005; Jackson and Eldridge, 1992; Oevelen et al., 2010; van Oevelen et al., 2006). Using two or more isotopic markers significantly increases model structure complexity and greatly increases model run time. This problem is compounded in situations where Monte Carlo methods are used to run the inverse analysis thousands of times (Kones et al., 2009; Niquil et al., 2012; van Oevelen et al., 2010). This has significant implications when attempting to add stable isotope information into food web models solved using the new linear inverse model-Markov chain Monte Carlo techniques (Kones et al., 2009; Niquil et al., 2012).

Therefore, the goal of this study was to find a way to incorporate information from multiple stable isotope elements (i.e., ^{13}C, ^{15}N, etc.) into food web models using the LIM-MCMC technique, with minimum added complexity. In order to do this, we used the R package SIAR (Stable Isotope Analysis in R; Parnell et al., 2010) to analyze Bayesian mixing models using $\delta^{13}C$ and $\delta^{15}N$ data to estimate food source distributions of the compartments in an inverse food web model of an intertidal seagrass bed. This information was then integrated into the LIM-MCMC food web model. Results of this model were compared with a corresponding model of the same system that excluded the isotope information obtained with the SIAR mixing models in order to investigate the effects of the added stable isotope information.

2. Methods

2.1. Marennes-Oléron Bay study site and model data

The seagrass system studied was an intertidal *Zostera noltii* meadow located in Marennes-Oléron Bay, on the Atlantic coast of France (45°54′ N, 1°12′ W) (Fig. 1). This is a semi-enclosed, macrotidal bay, which receives freshwater inputs from the Charente River (15–500 $m^3\ s^{-1}$). The seagrass bed studied extends for 15 km along the eastern shore of Oléron Island, and is 1.5 km at its widest.

Primary producer biomass, benthic consumer biomass, and stable isotope data used in this model were obtained from (Lebreton et al., 2009, 2012). Sampling was conducted at two stations (a high flat station and a low flat station) in 2006 and 2007 (Fig. 1) and the results were averaged (Table 1). Each station was a homogeneous area of 100 m^2 parallel to the coastline, about 250 m from the upper and lower limits of the seagrass bed, respectively. The stations were each broken up into 100 plots of 1 m^2 for sampling. Both sampling sites were exposed at every low tide, with the higher in elevation of the two sites being exposed for 5 h longer on average (Lebreton et al., 2009). Average emersion times on the seagrass bed were computed for this study using bathymetric data and tidal measurements, and those processes (i.e., phytoplankton production, bird grazing, zooplankton grazing, etc.) affected by the tidal cycle were scaled accordingly in the food web model.

2.2. Linear inverse model (LIM-MCMC) formulation

Two inverse food web models were built to track the flow of carbon through the seagrass food web on an annual basis, with units of $mgC\ m^{-2}\ d^{-1}$. The first model (Traditional LIM) included all available data, with the exception of the diet constraints formed from the stable isotope mixing models. The second LIM (Isotope LIM) was identical to the Traditional LIM, but included the SIAR diet constraints. Both models were identical in structure, and intended to model the same Marennes-Oleron intertidal seagrass bed.

First, an *a priori* topological model was formulated of the food web based on local expert knowledge and previous studies (Leguerrier et al., 2003, 2004), defining the compartments and all probable connections between them. All macrofaunal species sampled in the system were included which had a biomass of at least 0.05 g ash-free dry weight m^{-2}. This biomass threshold value resulted in 96.5% of the total measured biomass during sampling being included in the inverse food web model. The benthic and pelagic fauna of the system were parsed into compartments based on similarity of species-specific characteristics such as taxonomy, habitat, known feeding habits, known predators, and stable isotope ($\delta^{13}C$ and $\delta^{15}N$) values. Priority was placed on aggregating species into the compartments in such a way so as to balance between maintaining the true trophic complexity of the ecosystem versus the need to keep the model simple enough that solutions could be produced in a timely manner. As the complexity of the model scales exponentially with the number of compartments, some aggregation was necessary. However, loss in precision of stable isotope data due to aggregation of species with dissimilar signatures was considered to be undesirable for the mixing models, and was

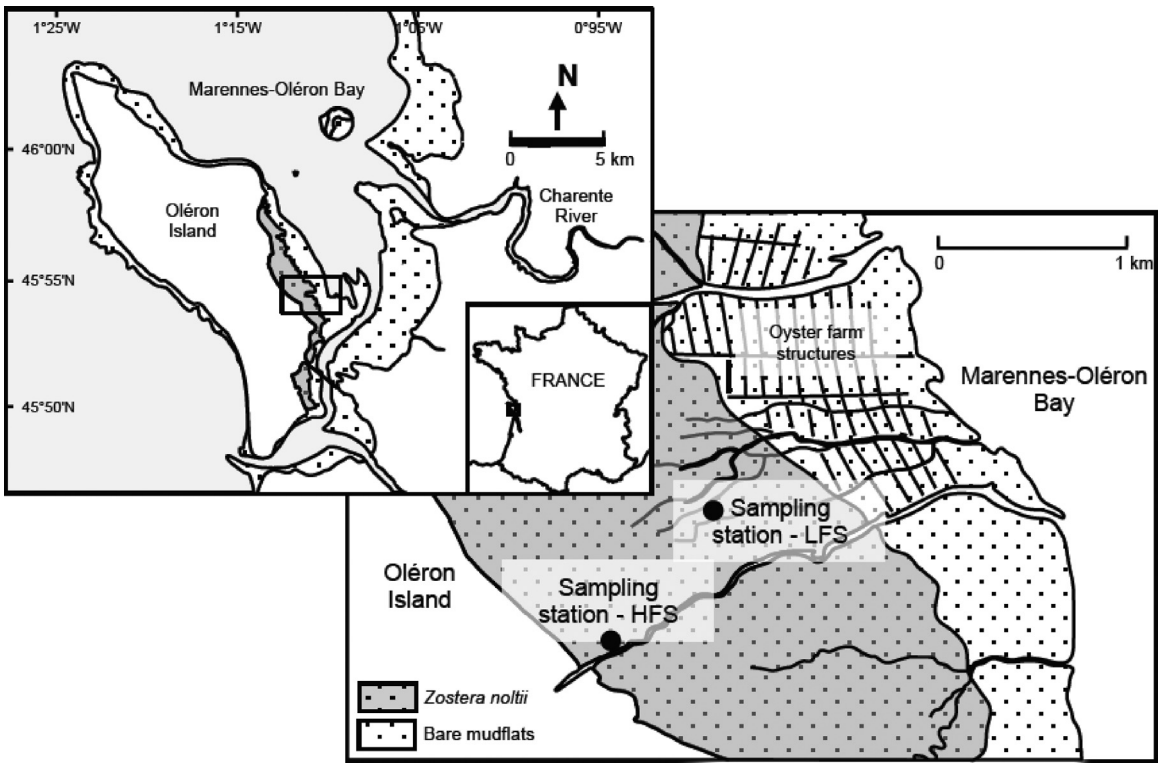

Fig. 1. Overview of Marennes-Oléron Estuary study site, including the intertidal seagrass bed that was modeled. Sampling locations indicated as HFS (High Flat Site) and LFS (Low Flat Site).

therefore avoided. Previous studies found that *a priori* model aggregation at low trophic levels has a greater effect on inverse model results than does aggregation of higher trophic levels (Johnson et al., 2009). In light of these results, primary producers, bacteria, and non-living carbon pools (e.g., dissolved organic carbon) were each given their own compartment. The resulting *a priori* food web model consisted of 26 compartments (23 living, 3 detrital) (Table 1) and 175 flows among compartments (Table 2).

The Traditional LIM and Isotope LIM were run using a Matlab routine that was a translation of the R packages limSolve and

Table 1
Food web compartments, along with their biomasses and stable isotope values used in the Traditional and Isotope LIMs.

Compartment	Compartment abbreviation	Biomass (mgC m^{-2})	δ^{13}C mean	δ^{13}C SD	δ^{15}N mean	δ^{15}N SD
Autotrophs						
Microphytobenthos	mpb	9250	−14.00	1.07	5.68	1.29
Zostera noltii	zos	6133	−10.98	1.06	8.46	1.53
Phytoplankton	phy	254.5	−23.70	2.37	4.90	0.49
Detritus						
Dissolved organic carbon	doc	1850	–	–	–	–
Sediment organic matter	som	27,560	−19.00	0.92	5.80	1.08
Particulate organic matter	pom	1044	−21.09	2.84	5.80	1.08
Heterotrophs						
Benthic Bacteria	bba	4718	–	–	–	–
Pelagic Bacteria	pba	157.3	–	–	–	–
Zooplankton	zoo	160.0	−24.35	2.43	7.39	0.74
Hydrobia ulvae	hyd	3752	−12.02	1.03	9.73	0.64
Nematodes	nem	2748	−12.83	0.61	9.80	0.73
Tapes spp.	tap	844.1	−16.94	1.79	9.15	0.79
Cerastoderma edule	cer	352.5	−16.99	1.19	9.83	0.97
Copepods	cop	359.0	−15.45	1.10	7.80	0.42
Gastropod grazers	gas	325.0	−11.50	1.11	10.18	1.29
Scrobicularia plana	scr	258.3	−14.28	0.71	9.98	1.06
Mytilus galoprovincialis	myt	127.1	−18.14	1.86	9.47	0.75
Abra spp.	abr	69.59	−13.52	1.07	11.47	1.91
Macoma balthica	mac	48.31	−13.38	0.53	11.07	2.23
Cerebratulus marginatus	ceb	14.22	−14.67	2.24	10.00	0.42
Carcinus maenas	car	25.96	−12.58	0.82	11.44	0.46
Crangon crangon	cra	10.66	−12.99	1.02	12.92	0.59
Notomastus latericeus	not	18.10	−13.87	1.16	13.10	2.18
Arenicola marina	are	11.15	−13.68	0.58	11.31	0.14
Fish	fsh	195.0	−15.11	3.29	13.08	2.14
Birds	brd	7.00	–	–	–	–

Table 2
SIAR-derived dietary contribution matrix. Lower and upper bounds of the 90% credible intervals are given, with consumers by row and prey items by column. Values are in units of percent contribution to total diet.

Isotope % diet matrix	Microalgae	*Zostera noltii*	Phytoplankton	Benthic Bacteria	Pelagic Bacteria	Zooplankton	*Abra* spp.	*Arenicola marina*	Birds	*Carcinus maenas*	*Cerastoderma edule*	*Cerebratulus marginatus*	Copepods	*Crangon crangon*
Abra spp	0–60	21–69												
Carcinus maenas						0–8	0–13	0–13			0–10	0–13	0–15	0–13
Cerastoderma edule	28–59		0–23											
Cerebratulus marginatus	1–37	0–30											0–42	
Crangon crangon						0–8	0–13	0–13		0–14	0–12	0–14	0–17	
Scrobicularia plana	79–96		0–11											
Tapes spp.	39–65		0–22											
Mytilus galoprovincialis	22–52		10–55											
Hydrobia ulvae	12–53	34–70		0–24										
Gastropod grazers	21–34	59–83		0–14										
Arenicola marina	0–41	21–60		21–56										
Copepods	38–98			2–62										

Fish	Gastropod grazers	*Hydrobia ulvae*	*Macoma balthica*	*Mytilus galoprovincialis*	Nematodes	*Notomastus latericeus*	*Scrobicularia plana*	*Tapes* spp.	DOC	POM	SOM
											9–45
0–10	0–21	0–20	0–14	0–10	0–18	0–11	0–14	0–11			0–15
										0–40	1–54
						0–35				5–42	
	0–19	0–18	0–13	0–11	0–17	0–11	0–14	0–12			0–14
										0–16	
										17–60	
										2–55	
											0–16
											0–11

xsample (Kones et al., 2009; Van den Meersche et al., 2009; van Oevelen et al., 2010). The routine uses a Markov Chain Monte Carlo (MCMC) algorithm to sample the LIM solution space using random jumps of a user-defined length. A "mirror" algorithm within the Matlab program creates a set of hyperplanes that form a convex solution space based on the equality and inequality constraints, out of which the sampling procedure cannot exit (Van den Meersche et al., 2009). These hyperplanes act as mirrors, which the random jumps are reflected by, and that ensure the samples are always taken from within the LIM feasible solution space. This procedure reduces the number of iterations required to fully characterize the solution space when compared with a solution procedure whose searching is not constrained to within the feasible solution space, as all samples of the mirror algorithm procedure are feasible solutions. Adequate sampling of the solution space and convergence was ensured through visual inspection of the sampling and results for each flow of the food web model. Note that the models were solved using the LIM-MCMC technique as described above, but will be referred to as the Traditional LIM and Isotope LIM for simplicity.

2.3. Stable isotope mixing models

The analytical precision of the stable isotope measurements was <0.15‰ and <0.2‰ for δ^{13}C and δ^{15}N values, respectively (Lebreton et al., 2012). Trophic enrichment factors used were 0.5‰ ± 0.5 for δ^{13}C and 2.5‰ ± 1.0 for δ^{15}N (Vander Zanden and Rasmussen, 2001).

The SIAR isotopic mixing model (Parnell et al., 2010) was used to characterize the proportions of food sources used by the consumers in the seagrass bed. SIAR is an open-source R package that uses Bayesian inference to address natural variation and uncertainty of stable isotope data in order to generate probability distributions of food source contributions as percentages of the total diet. SIAR allows for multiple dietary sources, incorporates variability in source, consumer and trophic enrichment factors. As a result, output probability estimates reflect uncertainties in the data better than previous mixing models (Parnell et al., 2010; Phillips and Gregg, 2001, 2003; Phillips et al., 2005). A critical assumption of isotope mixing models is that all food sources are included in the analysis. Excluding a food source will bias the apparent proportions of the other sources that were included in the analysis, and may yield a diet with apparent food source proportions inconsistent with the observed isotopic composition of the consumer (Parnell et al., 2012; Phillips, 2012). In order to meet this assumption, SIAR mixing models were only run for those LIM compartments whose food sources all had both δ^{13}C and δ^{15}N values. Models were not run for those LIM compartments whose food sources were not all described by both δ^{13}C and δ^{15}N data. For example, because the fish in the seagrass bed are known to be transitory, it cannot be assumed that all of their food sources are described by isotope data only collected from the within the seagrass bed. SIAR mixing models were therefore not run for this compartment. Of the 20 heterotrophic compartments in the LIM for which mixing models could potentially be used, 12 compartments met the assumptions required for a SIAR model to be run (Table 2). The 5% and 95% credible bounds of the generated probability density functions (PDF), expressed as percent contribution to the mixture for each food source, were recorded and used as input to the inverse model, as explained below. Credible intervals are used in Bayesian statistics to define the domain of *a posteriori* probability distribution used for interval estimation (e.g., if the 0.90 CI of a contribution value ranges from A to B, it means that there is a 90% chance that the contribution value lies between A and B) (Lebreton et al., 2012).

2.4. Incorporation of mixing model data into the food web model

The 5% and 95% credible bounds of the PDF for each food source were used as lower and upper bounds, respectively, to constrain the relative contributions of each food source to the 12 consumer compartments modeled using SIAR. In order to be incorporated into the food web model, these lower and upper bounds were transformed into linear inequalities of the form:

$$\text{lower bound} : C_{i,j} - l \times \Sigma C_{.,j} \geq 0$$

$$\text{upper bound} : h \times \Sigma C_{.,j} - C_{i,j} \geq 0$$

where $C_{i,j}$ is the flow of carbon from source i to consumer j, $\sum C_{.j}$ is the sum of all source flows to consumer j, l is the 5% credible bound for % mixture contribution, and h is the 95% credible bound for % mixture contribution. Using this methodology, if consumer j had three potential food sources, six inequalities were entered into the food web model to describe consumer j's diet. Note that while the food web model used carbon as the currency for mass flow, and these isotopic inequalities were written following this form, the values were informed by both δ^{13}C and δ^{15}N data via the SIAR modeling process.

2.5. Investigating effects of isotopic constraints on the food web model

Two versions of the food web model were created to investigate the effects of using isotopic constraints on the estimated mass flows among compartments within the food web. A first model (Traditional LIM) was built using all available data except the isotopic constraints. The second model (Isotope LIM) was identical to the first model, but included the SIAR-derived isotopic constraints. Each model was run for 50,000 solutions using the LIM-MCMC technique, and convergence to the marginal probability density function (mPDF) for individual flows was verified for both models. Non-convergence manifests itself as a drift in the mPDF with increased iterations (Kones et al., 2009).

Network indices were calculated for both food web models following the techniques of ecological network analysis (ENA) (Baird et al., 2009; Christian et al., 2009; Ulanowicz, 2004). These indices describe ecosystem network properties, interactions, and emergent properties of the system that are not otherwise directly observable (Fath et al., 2007). Indices computed were total system throughput, average path length, internal ascendency, internal development capacity, ascendency, development capacity, Finn cycling index and the comprehensive cycling index (Baird et al., 2004; Ulanowicz, 2004).

3. Results

3.1. SIAR mixing models

SIAR mixing models for the 12 consumer compartments whose food sources were fully described with δ^{13}C and δ^{15}N data resulted in probability distributions of food source proportions for each compartment. The 5% and 95% credible bounds for each potential food source were used as lower and upper bounds of relative contribution to the consumer diet. These resulting 90% credible intervals used in the LIM-MCMC are shown in Table 2.

3.2. Effects of isotopic constraints on the food web model

Sixty-four of the 175 flows in the Isotope LIM (Fig. 2) were constrained using SIAR-derived dietary constraints. The mean value for each flow and the corresponding 90% interquantile range (95%

Table 3
Flow means and 90% interquantile ranges of the Traditional and Isotope LIMs. Statistics are calculated with $n = 50{,}000$ for each model (the number of Monte-Carlo simulations). 90% interquantile ranges are calculated as the 95% quantile value minus the 5% interquantile value. Units are mgC m^{-2} d^{-1}. Each flow is composed of the abbreviation of the source compartment (see Table 1) TO the abbreviation of the sink compartment. gpp, gross primary production; imp, import; exp, export; res, respiration.

Flow (sourceTOsink)		Traditional model		Isotopic model	
		Mean	90% interquantile range	Mean	90% interquantile range
1	gppTOmpb	1357	339	1355	338
2	gppTOzos	55.0	19.9	55.3	13.4
3	gppTOphy	58.4	43.9	57.6	45.5
4	impTOpba	88.5	16.0	88.4	15.9
5	impTOphy	150	21.4	150	21.6
6	impTOzoo	94.0	13.6	94.0	13.7
7	impTOfsh	160	96.6	159	96.4
8	impTObrd	4.6	2.7	4.7	2.5
9	impTOpom	598	106	598	106
10	impTOdoc	1067	185	1064	186
11	mpbTOres	323	229	324	228
12	mpbTOdoc	695	214	695	214
13	mpbTObba	142	235	146	208
14	**mpbTOabr**[a]	**0.8**	**1.9**	**1.0**	**0.8**
15	**mpbTOare**[b]	**0.2**	**0.4**	**0.1**	**0.2**
16	mpbTObrd[b]	7.9	19.5	0.2	0.4
17	**mpbTOcer**[b]	**2.6**	**6.4**	**4.5**	**3.3**
18	**mpbTOceb**	**0.0**	**0.1**	**0.0**	**0.1**
19	**mpbTOcop**[b]	**21.7**	**43.2**	**30.8**	**28.0**
20	mpbTOfsh	40.0	7.2	40.0	7.2
21	**mpbTOgas**[a]	**2.0**	**4.8**	**1.5**	**0.9**
22	**mpbTOhyd**[a]	**47.2**	**114**	**52.2**	**26**
23	mpbTOmac	0.2	0.6	0.2	0.6
24	**mpbTOmyt**[a]	**1.2**	**2.8**	**1.5**	**1.2**
25	mpbTOnem[b]	63.8	150	41.7	101
26	mpbTOnot	0.4	0.8	0.4	0.8
27	**mpbTOscr**[b]	**2.0**	**4.7**	**5.3**	**1.9**
28	**mpbTOtap**[b]	**6.9**	**15.7**	**10.6**	**6.2**
29	zosTOres[b]	10.9	15.2	7.5	13.4
30	zosTOdoc[b]	2.0	2.4	0.9	0.3
31	zosTOexp[b]	5.7	15.2	0.1	0.2
32	zosTOsom[b]	5.8	15.6	0.1	0.2
33	**zosTOabr**[b]	**0.8**	**1.8**	**0.6**	**0.3**
34	**zosTOare**	**0.2**	**0.4**	**0.2**	**0.1**
35	zosTObrd[b]	22.8	23.7	0.4	0.5
36	**zosTOceb**[b]	**0.0**	**0.1**	**0.0**	**0.0**
37	**zosTOgas**[b]	**1.6**	**4.1**	**3.5**	**0.5**
38	**zosTOhyd**[b]	**5.4**	**14.7**	**42.2**	**0.5**
39	phyTOres	11.3	18.2	11.2	18.2
40	phyTOdoc	6.1	4.2	6.0	4.4
41	phyTOexp	139	21.3	140	21.5
42	phyTOpom[a]	24.2	44.5	29.5	48.6
43	**phyTOcer**[b]	**2.6**	**6.3**	**1.2**	**2.2**
44	phyTOmac	0.2	0.6	0.2	0.6
45	**phytOmyt**[b]	**1.2**	**2.8**	**0.8**	**1.4**
46	**phyTOscr**[b]	**2.0**	**4.6**	**0.3**	**0.6**
47	**phyTOtap**[b]	**6.5**	**15.1**	**2.2**	**4.2**
48	phyTOzoo[a]	14.6	35.0	16.2	38.5
49	docTOexp	1036	185	1038	185
50	docTOpba	72.5	162	72.8	162
51	docTObba	937	426	937	423
52	pomTOexp	348	456	367	456
53	pomTOsom	436	403	433	407
54	**pomTOcer**[a]	**2.6**	**6.5**	**2.0**	**3.7**
55	pomTOmac	0.2	0.6	0.2	0.6
56	**pomTOmyt**[a]	**1.3**	**2.8**	**1.5**	**1.9**
57	pomTOpba	87.9	176	86.2	174
58	**pomTOscr**[b]	**2.1**	**4.6**	**0.5**	**0.9**
59	**pomTOtap**	**7.1**	**15.9**	**7.7**	**7.0**
60	pomTOzoo	21.6	54.1	21.1	53.5
61	somTOexp	167	392	172	398
62	somTOpom	166	399	169	401
63	**somTOabr**[a]	**0.8**	**1.9**	**0.7**	**0.7**
64	somTObba	237	416	218	397
65	**somTOcar**	**0.1**	**0.2**	**0.1**	**0.1**
66	somTOceb[a]	0.0	0.1	0.0	0.1
67	**somTOcer**	**2.6**	**6.4**	**2.7**	**4.5**
68	**somTOcra**	**0.1**	**0.2**	**0.1**	**0.1**
69	**somTOgas**[b]	**2.0**	**4.8**	**0.3**	**0.6**
70	**somTOhyd**[b]	**49.0**	**118**	**10.9**	**18**
71	somTOmac	0.2	0.6	0.2	0.6
72	somTOnot	0.4	0.8	0.4	0.8

Table 3 (*Continued*)

Flow (sourceTOsink)		Traditional model		Isotopic model	
		Mean	90% interquantile range	Mean	90% interquantile range
73	bbaTOres	626	234	623	220
74	bbaTOdoc	103	50.9	103	50.8
75	**bbaTOare**[a]	**0.2**	**0.4**	**0.2**	**0.2**
76	**bbaTOcop**[b]	**25.3**	**44.0**	**16.2**	**26.6**
77	**bbaTOgas**[b]	**2.0**	**4.8**	**0.4**	**0.7**
78	**bbaTOhyd**[b]	**72.0**	**135**	**18.5**	**24**
79	bbaTOnem[a]	487	170	540	107
80	pbaTOres	38.7	92.4	38.7	92.5
81	pbaTOdoc	44.0	99.9	43.4	99.2
82	pbaTOexp	90.3	16.0	90.3	16.0
83	pbaTOzoo	75.9	62.3	75.1	62.7
84	zooTOres	51.7	16.6	51.8	16.5
85	zooTOdoc	35.4	32.7	35.6	32.8
86	zooTOexp	88.0	13.7	88.0	13.7
87	zooTOpom	10.4	21.4	10.4	21.4
88	**zooTOcar**[b]	**0.1**	**0.2**	**0.0**	**0.1**
89	**zooTOcra**[b]	**0.1**	**0.2**	**0.0**	**0.1**
90	zooTOfsh	20.5	26.7	20.5	26.7
91	abrTOres	1.3	0.2	1.3	0.2
92	abrTOsom[a]	0.9	0.8	0.7	0.7
93	**abrTOcar**	**0.1**	**0.2**	**0.1**	**0.1**
94	**abrTOcra**	**0.1**	**0.2**	**0.1**	**0.1**
95	abrTOfsh	0.1	0.2	0.1	0.2
96	areTOres	0.2	0.0	0.2	0.0
97	areTOsom	0.2	0.1	0.2	0.1
98	areTObrd[a]	0.0	0.0	0.0	0.0
99	**areTOcar**[a]	**0.0**	**0.0**	**0.0**	**0.0**
100	**areTOcra**[a]	**0.0**	**0.0**	**0.0**	**0.0**
101	areTOfsh	0.0	0.0	0.0	0.0
102	brdTOres[b]	24.3	29.1	0.7	1.3
103	brdTOsom[b]	14.6	19.2	0.4	0.6
104	brdTOexp	4.5	2.7	4.3	2.5
105	carTOres	0.4	0.1	0.4	0.1
106	carTOsom	0.4	0.2	0.4	0.2
107	**carTOcra**[b]	**0.0**	**0.1**	**0.1**	**0.1**
108	carTofsh[a]	0.1	0.1	0.1	0.1
109	cerTOres	5.3	0.6	5.3	0.6
110	cerTOsom	3.8	3.2	3.8	3.2
111	**cerTOcar**[b]	**0.1**	**0.2**	**0.0**	**0.1**
112	**cerTOcra**[a]	**0.1**	**0.2**	**0.1**	**0.1**
113	cerTOfsh	1.1	0.4	1.1	0.3
114	cebTOres	0.1	0.0	0.1	0.0
115	cebTOsom	0.1	0.1	0.1	0.0
116	**cebTOcar**	**0.0**	**0.0**	**0.0**	**0.0**
117	**cebTOcra**	**0.0**	**0.0**	**0.0**	**0.0**
118	cebTOfsh	0.0	0.0	0.0	0.0
119	copTOres	26.7	3.4	26.7	3.4
120	copTOdoc	12.4	17.0	12.5	17.0
121	copTOsom	7.7	16.3	7.7	16.3
122	**copTOcar**	**0.1**	**0.2**	**0.1**	**0.1**
123	copTOceb[a]	0.0	0.1	0.0	0.1
124	**copTOcra**[a]	**0.1**	**0.2**	**0.1**	**0.1**
125	craTOres	0.4	0.1	0.4	0.1
126	craTOsom	0.4	0.2	0.4	0.2
127	**craTOcar**[a]	**0.0**	**0.1**	**0.0**	**0.1**
128	craTOfsh[a]	0.0	0.1	0.0	0.1
129	fshTOres	160	79.6	164	74.6
130	fshTOpom	108	91.2	112	92.9
131	fshTOexp	172	95.4	174	95.3
132	**fshTOcar**[b]	**0.1**	**0.2**	**0.0**	**0.1**
133	gasTOres[a]	3.5	0.9	3.0	0.3
134	gasTOsom[b]	2.5	2.1	1.3	0.4
135	**gasTOcar**[b]	**0.1**	**0.2**	**0.1**	**0.2**
136	**gasTOcra**[b]	**0.1**	**0.2**	**0.1**	**0.2**
137	gasTOfsh[a]	1.4	0.5	1.2	0.4
138	hydTOres[a]	83.0	18.1	71.9	0.6
139	hydTOsom[b]	59.9	49.8	26.2	0.7
140	hydTObrd[b]	8.1	19.8	0.1	0.3
141	**hydTOcar**[b]	**0.1**	**0.2**	**0.1**	**0.2**
142	**hydTOcra**[a]	**0.1**	**0.2**	**0.1**	**0.1**
143	hydTOfsh[a]	22.3	22.6	25.4	0.7
144	macTOres	0.5	0.0	0.5	0.0
145	macTOsom	0.3	0.3	0.3	0.3
146	**macTOcar**[a]	**0.0**	**0.1**	**0.0**	**0.1**
147	**macTOcra**[a]	**0.0**	**0.1**	**0.0**	**0.1**

Table 3 (*Continued*)

Flow (sourceTOsink)		Traditional model		Isotopic model	
		Mean	90% interquantile range	Mean	90% interquantile range
148	macTOfsh[a]	0.0	0.1	0.0	0.1
149	mytTOres	1.9	0.2	1.9	0.2
150	mytTOsom	1.4	1.2	1.4	1.2
151	**mytTOcar**[b]	**0.1**	**0.2**	**0.0**	**0.1**
152	**mytTOcra**[b]	**0.1**	**0.2**	**0.0**	**0.1**
153	mytTOfsh[a]	0.3	0.3	0.3	0.2
154	nemTOres	198	71.4	207	49.7
155	nemTOdoc	80.8	158	87.4	166
156	nemTOsom	80.8	158	88.5	167
157	**nemTOcar**[b]	**0.1**	**0.2**	**0.1**	**0.2**
158	**nemTOceb**	**0.0**	**0.1**	**0.0**	**0.1**
159	nemTOcra[a]	0.1	0.2	0.1	0.1
160	nemTOfsh	192	87.9	199	85.8
161	notTOres	0.4	0.1	0.4	0.1
162	notTOsom	0.3	0.3	0.3	0.3
163	**notTOcar**[a]	**0.0**	**0.1**	**0.0**	**0.1**
164	**notTOcra**[a]	**0.0**	**0.1**	**0.0**	**0.1**
165	notTOfsh[a]	0.1	0.1	0.0	0.1
166	scrTOres	3.2	0.2	3.2	0.2
167	scrTOsom	2.2	1.9	2.2	1.9
168	**scrTOcar**	**0.1**	**0.2**	**0.1**	**0.1**
169	**scrTOcra**	**0.1**	**0.2**	**0.1**	**0.1**
170	scrTOfsh	0.6	0.3	0.6	0.2
171	tapTOres	10.8	0.7	10.8	0.7
172	tapTOsom	7.6	6.4	7.6	6.4
173	**tapTOcar**[b]	**0.1**	**0.2**	**0.0**	**0.1**
174	**tapTOcra**[a]	**0.1**	**0.2**	**0.1**	**0.1**
175	tapTOfsh	2.1	0.6	2.1	0.5

Bold: flow with corresponding SIAR diet constraint.

[a] Means of Isotope and Traditional LIM > 10% different.

[b] Means of Isotope and Traditional LIM > 25% different.

credible interval value – 5% credible interval value) are presented in Table 3. Seventy-nine (45%) and 43 (24%) of the means for the 175 flows were different between the Isotope and the Traditional LIMs by at least 10% and 25%, respectively (Table 3). Of the 64 flows which were constrained with SIAR-derived dietary constraints, 50 had their means change by at least 10%, and 31 had their means change by at least 25%. On average, all flows had a 23% absolute mean difference for the Isotope LIM in comparison with the Traditional; similarly the 90% interquantile ranges of the flows were reduced by 26% for the Isotope LIM in comparison with the Traditional LIM

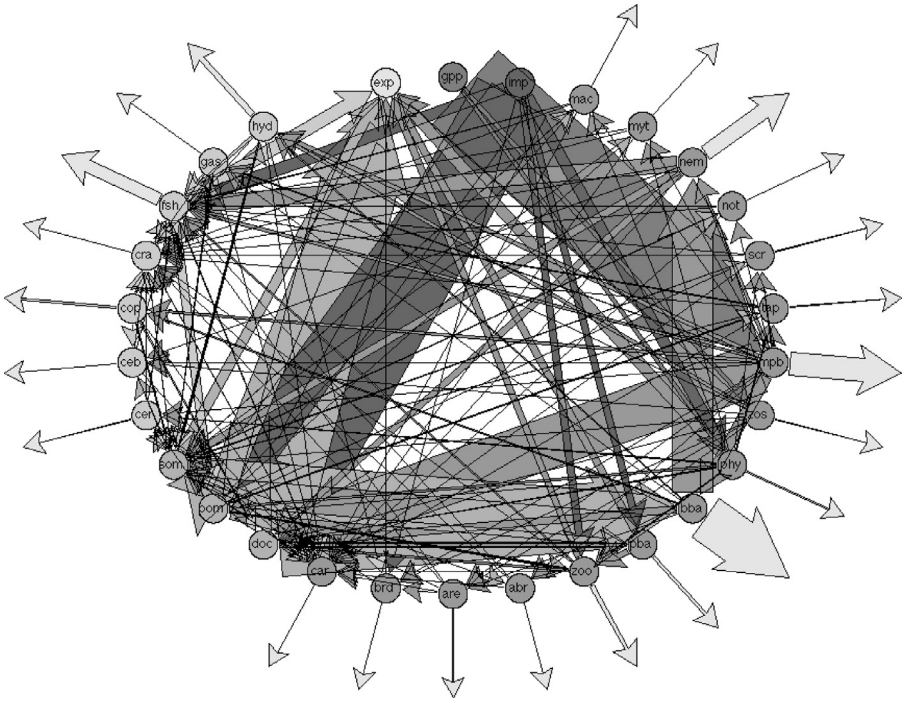

Fig. 2. Food web diagram of the Marennes-Oléron intertidal seagrass system, formed using the mean flows from the Isotope LIM. Width of arrows corresponds to relative magnitude of flow in units of mgC m^{-2} d^{-1}. Arrows pointing away from center of the web represent respiration and exports from the system. Abbreviations for food web compartments are in Table 1.

Table 4
Comparison of means and 90% interquantile ranges for the Traditional and Isotope LIMs. The absolute mean difference for each flow was calculated as the absolute value of the difference between Traditional and Isotope LIM mean flow values. Negative values indicate a reduction in the interquantile range of the Isotope LIM when compared with the Traditional LIM.

Average change in statistic after incorporation of isotope information					
All food web flows		Flows with SIAR constraints		Flows without SIAR constraints	
Absolute mean difference	90% interquantile range	Absolute mean difference	90% interquantile range	Absolute mean difference	90% interquantile range
23%	−26%	42%	−45%	12%	−15%

Table 5
Comparison of the means and 90% interquantile (IQ) ranges of the Ecological Network Analysis indices for each of the models. Negative values for the percent change of 90% IQ range represent a reduction in the range of the Isotope LIM when compared with the Traditional LIM.

ENA index	Traditional LIM		Isotope LIM		% change	
	Mean	90% IQ range	Mean	90% IQ range	Absolute mean difference	90% IQ range
Total system throughput	11,911	1392	11,801	1373	0.9%	−1.4%
Average path length	2.28	0.26	2.26	0.25	1.1%	−3.8%
Internal ascendency	9486	2372	9325	2369	1.7%	−0.1%
Internal development capacity	30,733	3860	30,047	3770	2.2%	−2.3%
Ascendency	19,111	2790	18,904	2762	1.1%	−1.0%
Development capacity	36,955	4510	36,219	4413	2.0%	−2.2%
Finn cycling index	0.052	0.041	0.051	0.043	0.7%	4.9%
Comprehensive cycling index	0.059	0.047	0.058	0.050	0.7%	6.4%

(Table 4). Flows constrained in the Isotope LIM using SIAR-derived diet constraints had, on average, a 42% absolute mean difference in comparison with the corresponding Traditional LIM flows, and their 90% interquantile ranges were reduced 45%. Additionally, the remaining 111 flows (those that were not directly constrained with SIAR-derived diet constraints in the Isotope LIM) had, on average, a 12% absolute mean difference, and 90% interquantile ranges were reduced by 15% on average.

All network indices (total system throughput, average path length, internal ascendency, internal development capacity, ascendency, development capacity, Finn cycling index and comprehensive cycling index) calculated from the Traditional and Isotope LIMs had small differences in their means (Table 5). Changes in the 90% interquantile ranges with the addition of the SIAR-derived isotope constraints in the Isotope LIM were small when compared with the Traditional LIM (Table 5).

4. Discussion

4.1. Comparison of single flows and integrative indices between LIMs

Both individual flows and integrative indices as calculated from ENA parameters were changed as a result of the addition of the SIAR-derived dietary constraints in the Isotope LIM. However, the comparison of the ENA indices showed smaller differences in the means, uncertainty (90% interquantile ranges), and marginal probability distributions between the Traditional and Isotope LIMs when compared to those differences between individual flows. This agrees with the findings of Kones et al. (2009), who found that whole network indices are better constrained and more robust than the food webs from which they are calculated. Differences between the two models were more apparent when looking at the individual flow level as compared to a more aggregate, whole system measure (i.e., ENA indices). This suggests that the integration of the stable isotope data has the largest effect when looking at specific flows within the food web. Linear inverse models are most often utilized to quantify systems with a large number of unknown flows and data deficiencies. The fact that the integrative indices calculated from the Traditional and Isotope LIMs show small differences supports the idea that the LIM-MCMC technique is a robust method for assessing whole-ecosystem properties, even in the absence of site-specific stable isotope data, following the findings of Kones et al. (2009).

Generally, the largest differences seen between the Traditional and Isotope LIMs were in those flows which were directly constrained by SIAR-derived diet constraints (Table 4). However, flows not directly constrained with isotope data were still affected, as evidenced by the reduced uncertainty and changes in means. This demonstrates the interconnected nature of the food web, as well as how constraining some flows with isotope data can have widespread effects on reducing uncertainty in LIM-MCMC models.

4.2. Integration of stable isotope data in food web models

The goal of this study was to find a way to incorporate information from multiple stable isotope elements (i.e., ^{13}C, ^{15}N, etc.) into food web models using the LIM-MCMC technique, with minimum added complexity. The technique of using SIAR-derived food source contribution constraints successfully integrated $\delta^{13}C$ and $\delta^{15}N$ information into the LIM-MCMC models. Analysis of LIM-MCMC output showed the Isotope LIM to be significantly different, as well as significantly more precise, than the Traditional LIM. Thus, the integration of $\delta^{13}C$ and $\delta^{15}N$ data into the food web model through isotope mixing model diet constraints succeeded in reducing the uncertainty of the food web model solution. van Oevelen et al. (2006) found, similarly, that inclusion of $\delta^{13}C$ data significantly constrained a conventional LIM of a benthic intertidal flat food web. This study built on this finding by simultaneously including stable isotope information from two markers ($\delta^{13}C$ and $\delta^{15}N$), as well as using stochastic techniques to fully describe the food web model solution space and associated uncertainty. While it is not a surprising result that the addition of further constraints to the model reduces the uncertainty and mPDFs, this had yet to be demonstrated with the use of Bayesian stable isotope mixing model constraints in a linear inverse model. This is significant, as the method introduced here combines two useful ecological modeling techniques available to ecologists. Additionally, the LIM-MCMC technique allowed for the investigation of what parts of the model were most (and least) constrained with the use of the mPDFs for each flow and integrative index.

The use of the SIAR mixing models allowed for incorporation of uncertainty in both the measured stable isotope values, as well as the fractionation factors. Incorporating the 90% credible intervals from the mixing models into the LIM-MCMC in the form of inequalities agrees well with conventional practices for building linear inverse models and is relatively simple to do, but comes at the cost of losing information regarding the tails of the marginal posterior distributions. Future models may choose to incorporate this information in a similar fashion to Hosack and Eldridge (2009), though this would add significant complexity. This methodology allows for data from multiple isotopic markers to be used in order to estimate contributions from all likely food sources to each consumer. It is well established that a multiple marker approach (δ^{13}C and δ^{15}N) is significantly more informative when estimating diet contributions when compared to a single marker (δ^{13}C or δ^{15}N) (Parnell et al., 2012; Phillips, 2012). Due to this, use of stable isotope mixing models in ecosystem-level food web studies can be advantageous for quantifying consumption flows. These same food web flows are often the most difficult to directly observe and measure as well, making isotopic mixing models a powerful tool for coupling with ecosystem-level food web models. This study used only two isotopic markers (δ^{13}C and δ^{15}N), as this was the only data available at the time, although the SIAR mixing models allow for incorporation of more than two (Parnell et al., 2010). However, use of isotopic mixing models utilizing more than three markers becomes problematic, as it is difficult to determine the model fit and visualize the mixing space (this would require > three dimensions) (Parnell et al., 2012).

Additionally, the use of the stable isotope mixing models helped validate the *a priori* food web model by verifying that the consumer diet networks were possible, and not missing a potential food source as indicated by the isotope data. While no statistical test exists for missing food sources (Parnell et al., 2012), property–property plots of food source isotope data (e.g. δ^{15}N vs. δ^{13}C) for food web compartments is a tool that ecologists can use to identify probable predator–prey relationships. As mentioned, multiple isotopic markers help to better elucidate these relationships. Perhaps most importantly, though, is the fact that the stable isotope data specifically constrain consumption flows, which are often the most difficult to obtain reliable data on. This difficulty in obtaining reliable data leads to many ecosystem network models using diet data not specific to the study site of interest, such as from databases like FishBase (www.fishbase.org) (Coll et al., 2011). This can be a dangerous practice, as it has been shown that there can be considerable inter-site variability in the diet of members of the same species. We recommend the use of local diet information in the construction of food web models, as can be provided by mixing models utilizing site-specific stable isotope markers. It is important to note that stable isotope data obtained from the literature or other sites is not useful when building a food web model, as values are site-specific and only comparable within the site and appropriate temporal period from which the stable isotope samples were gathered.

4.3. Effects of SIAR-derived food source constraints on the modeled food web

Integration of mixing model constraints into LIM-MCMC models address an obvious weakness of stable isotope mixing models: current commonly used mixing models do not take into account the availability of food sources (Parnell et al., 2010; Phillips and Gregg, 2003; Semmens et al., 2009). Mixture partitioning is dictated purely by the stable isotope signatures of the consumer and food sources, regardless of whether or not there are enough of those food sources in the system to support the level of consumption suggested by the mixing model. The LIM-MCMC model deals with this issue through mass balance of each compartment, and incorporating field-measured biomass estimates for each compartment into the model. This constrains the biomass of each compartment in the model, and therefore the amount available for consumption. While a simple concept, this is nonetheless an important attribute of ecosystem models, and an example of how the combination of isotope mixing models with inverse food web models is quite beneficial.

The use of the Markov-Chain Monte Carlo method (van Oevelen et al., 2010) to solve the models enabled the statistical comparison to be done between the Traditional and Isotope models. Previous techniques, which relied on minimization of an objective function to choose one answer for a model, did not allow for statistically rigorous comparisons between models (Vezina and Platt, 1988). Comparison of the mPDFs of each flow allowed for utilization of all solution data from the models, as well as taking into account the uncertainty associated with each flow. The same concept applied to the comparisons of the ENA indices. The LIM-MCMC technique also allows for the repeatability of model solutions, which is imperative for future comparative ecosystem studies.

Acknowledgments

The present study was done in partial fulfillment of a M.S. degree by Stephen R. Pacella through Oregon State University. The study was carried out at the University of La Rochelle, France and Oregon State University, United States, and partially funded by the European research programs PNEC/EC2CO (projects COMPECO and ORIQUART) and the Région Poitou Charentes through the CPER program. We are grateful to all of our colleagues who made data available and helped with the modeling process, including Boutheina Grami, Blanche Saint-Béat, and Geoffrey R. Hosack. This document has been subjected to review by the National Health and Environmental Effects Research Laboratory's Western Ecology Division and approved for publication. Approval does not signify that the contents reflects the views of the Agency, nor does mention of trade names or commercial products constitute endorsement or recommendation for use.

References

Baeta, A., Niquil, N., Marques, J.C., Patrício, J., 2011. Modelling the effects of eutrophication, mitigation measures and an extreme flood event on estuarine benthic food webs. Ecological Modelling 222, 1209–1221.

Baird, D., Asmus, H., Asmus, R., 2004. Energy flow of a boreal intertidal ecosystem, the Sylt-Rømø Bight. Marine Ecology Progress Series 279, 45–61.

Baird, D., Fath, B., Ulanowicz, R., Asmus, H., 2009. On the consequences of aggregation and balancing of networks on system properties derived from ecological network analysis. Ecological Modelling 279, 45–61.

Banašek-Richter, C., Cattin, M.-F., Bersier, L.-F., 2004. Sampling effects and the robustness of quantitative and qualitative food-web descriptors. Journal of Theoretical Biology 226, 23–32.

Breed, G., Jackson, G., Richardson, T., 2004. Sedimentation, carbon export and food web structure in the Mississippi River plume described by inverse analysis. Marine Ecology Progress Series 278, 35–51.

Christensen, V., Pauly, D., 1992. Ecopath II—a software for balancing steady-state ecosystem models and calculating network characteristics. Ecological Modelling 61, 169–185.

Christian, R., Brinson, M., Dame, J., Johnson, G., 2009. Ecological network analyses and their use for establishing reference domain in functional assessment of an estuary. Ecological Modelling 220, 3113–3122.

Coll, M., Schmidt, A., Romanuk, T., Lotze, H.K., 2011. Food-web structure of seagrass communities across different spatial scales and human impacts. PLoS ONE 6, e22591.

Daniels, R., Richardson, T., Ducklow, H., 2006. Food web structure and biogeochemical processes during oceanic phytoplankton blooms: an inverse model analysis. Deep Sea Research Part II: Topical Studies in Oceanography 53, 532–554.

Degré, D., Leguerrier, D., Armynot du Chatelet, E., Rzeznik, J., Auguet, J., Dupuy, C., Marquis, E., Fichet, D., Struski, C., Joyeux, E., 2006. Comparative analysis of the food webs of two intertidal mudflats during two seasons using inverse modelling: Aiguillon Cove and Brouage Mudflat, France. Estuarine, Coastal and Shelf Science 69, 107–124.

Donali, E., Olli, K., Heiskanen, A., Andersen, T., 1999. Carbon flow patterns in the planktonic food web of the Gulf of Riga, the Baltic Sea: a reconstruction by the inverse method. Journal of Marine Systems 23, 251–268.
Eldridge, P., Cifuentes, L., Kaldy, J., 2005. Development of a stable-isotope constraint system for estuarine food-web models. Marine Ecology Progress Series 303, 73–90.
Eldridge, P., Jackson, G., 1993. Benthic trophic dynamics in California coastal basin and continental slope communities inferred using inverse analysis. Marine Ecology Progress Series 99, 115–135.
Fath, B.D., Scharler, U.M., Ulanowicz, R.E., Hannon, B., 2007. Ecological network analysis: network construction. Ecological Modelling 208, 49–55.
Finn, J.T., Leschine, T.M., 1980. Does salt marsh fertilization enhance shellfish production? An application of flow analysis. Environmental Management 4 (3), 193–203.
Grami, B., Niquil, N., Sakka Hlaili, A., Gosselin, M., Hamel, D., Hadj Mabrouk, H., 2008. The plankton food web of the Bizerte Lagoon (South-western Mediterranean): II. Carbon steady-state modelling using inverse analysis. Estuarine. Coastal and Shelf Science 79, 101–113.
Grami, B., Rasconi, S., Niquil, N., Jobard, M., Saint-Béat, B., Sime-Ngando, T., 2011. Functional effects of parasites on food web properties during the spring diatom bloom in Lake Pavin: a linear inverse modeling analysis. PLoS ONE 6, e23273.
Hosack, G.R., Eldridge, P.M., 2009. Do microbial processes regulate the stability of a coral atoll's enclosed pelagic ecosystem? Ecological Modelling 220, 2665–2682.
Jackson, G., Eldridge, P., 1992. Food web analysis of a planktonic system off Southern California. Progress in Oceanography 30, 223–251.
Johnson, G., Niquil, N., Asmus, H., Bacher, C., 2009. The effects of aggregation on the performance of the inverse method and indicators of network analysis. Ecological Modelling 220, 3448–3464.
Kones, J., Soetaert, K., van Oevelen, D., Owino, J., 2009. Are network indices robust indicators of food web functioning? a Monte Carlo approach. Ecological Modelling 220, 370–382.
Kones, J., Soetaert, K., van Oevelen, D., Owino, J., Mavuti, K., 2006. Gaining insight into food webs reconstructed by the inverse method. Journal of Marine Systems 60, 153–166.
Lebreton, B., Richard, P., Galois, R., Radenac, G., Brahmia, A., Colli, G., Grouazel, M., André, C., Guillou, G., Blanchard, G.F., 2012. Food sources used by sediment meiofauna in an intertidal *Zostera noltii* seagrass bed: a seasonal stable isotope study. Marine Biology 159, 1537–1550.
Lebreton, B., Richard, P., Radenac, G., Bordes, M., Breret, M., Arnaud, C., Mornet, F., Blanchard, G., 2009. Are epiphytes a significant component of intertidal *Zostera noltii* beds? Aquatic Botany 91, 82–90.
Leguerrier, D., Degré, D., Niquil, N., 2007. Network analysis and inter-ecosystem comparison of two intertidal mudflat food webs (Brouage Mudflat and Aiguillon Cove, SW France). Estuarine, Coastal and Shelf Science 74, 403–418.
Leguerrier, D., Niquil, N., Boileau, N., Rzeznik, J., Sauriau, P., Le Moine, O., Bacher, C., 2003. Numerical analysis of the food web of an intertidal mudflat ecosystem on the Atlantic coast of France. Marine Ecology Progress Series 246, 17–37.
Leguerrier, D., Niquil, N., Petiau, A., Bodoy, A., 2004. Modeling the impact of oyster culture on a mudflat food web in Marennes-Oléron Bay (France). Marine Ecology Progress Series 273, 147–161.
Leslie, H.M., McLeod, K.L., 2007. Confronting the challenges of implementing marine ecosystem-based management. Frontiers in Ecology and the Environment 5, 540–548.
Moore, J., Semmens, B., 2008. Incorporating uncertainty and prior information into stable isotope mixing models. Ecology Letters 11, 470–480.
Navarro, J., Coll, M., Louzao, M., Palomera, I., Delgado, A., Forero, M., 2011. Comparison of ecosystem modelling and isotopic approach as ecological tools to investigate food webs in the NW Mediterranean Sea. Journal of Experimental Marine Biology and Ecology 401, 97–104.
Niquil, N., Bartoli, G., Urabe, J., Jackson, G., Legendre, L., Dupuy, C., Kumagai, M., 2006. Carbon steady-state model of the planktonic food web of Lake Biwa, Japan. Freshwater Biology 51, 1570–1585.
Niquil, N., Chaumillon, E., Johnson, G.A., Bertin, X., Grami, B., David, V., Bacher, C., Asmus, H., Baird, D., Asmus, R., 2012. The effect of physical drivers on ecosystem indices derived from ecological network analysis: comparison across estuarine ecosystems. Estuarine, Coastal and Shelf Science 108, 132–143.
Niquil, N., Jackson, G., Legendre, L., Delesalle, B., 1998. Inverse model analysis of the planktonic food web of Takapoto Atoll (French Polynesia). Marine Ecology Progress Series 165, 17–29.
Oevelen, D., Meersche, K., Meysman, F.J.R., Soetaert, K., Middelburg, J.J., Vézina, A.F., 2010. Quantifying food web flows using linear inverse models. Ecosystems 13, 32–45.
Parnell, A., Inger, R., Bearhop, S., Jackson, A., 2010. Source partitioning using stable isotopes: coping with too much variation. PLoS ONE 5, e9672.
Parnell, A.C., Phillips, D.L., Bearhop, S., 2012. Bayesian Stable Isotope Mixing Models. arXiv:1209.6457v1.
Pauly, D., 2000. Ecopath, ecosim, and ecospace as tools for evaluating ecosystem impact of fisheries. ICES Journal of Marine Science 57, 697–706.
Phillips, D., Gregg, J., 2001. Uncertainty in source partitioning using stable isotopes. Oecologia 127, 171–179.
Phillips, D., Gregg, J., 2003. Source partitioning using stable isotopes: coping with too many sources. Oecologia 136, 261–269.
Phillips, D., Newsome, S., Gregg, J., 2005. Combining sources in stable isotope mixing models: alternative methods. Oecologia 144, 520–527.
Phillips, D.L., 2012. Converting isotope values to diet composition: the use of mixing models. Journal of Mammalogy 93, 342–352.
Post, D., 2002. Using stable isotopes to estimate trophic position: models, methods, and assumptions. Ecology 83, 703–718.
Semmens, B.X., Moore, J.W., Ward, E.J., 2009. Improving Bayesian isotope mixing models: a response to Jacksonet al. (2009). Ecology Letters 12, E6–E8.
Ulanowicz, R., 2004. Quantitative methods for ecological network analysis. Computational Biology and Chemistry 28, 321–339.
Van den Meersche, K., Soetaert, K., van Oevelen, D., 2009. xsample(): an R function for sampling linear inverse problems. Journal of Statistical Software, Code Snippets 30, 1–15.
van Oevelen, D., Soetaert, K., Middelburg, J., Herman, P., Moodley, L., Hamels, I., Moens, T., Heip, C., 2006. Carbon flows through a benthic food web: integrating biomass, isotope and tracer data. Journal of Marine Research 64, 453–482.
van Oevelen, D., Van den Meersche, K., Meysman, F., Soetaert, K., Middelburg, J., Vézina, A., 2010. Quantifying food web flows using linear inverse models. Ecosystems 13, 32–45.
Vander Zanden, M.J., Rasmussen, J.B., 2001. Variation in $\delta^{15}N$ and $\delta^{13}C$ trophic fractionation: implications for aquatic food web studies. Limnology and Oceanography 46, 2061–2066.
Vezina, A., Platt, T., 1988. Food web dynamics in the ocean. 1. Best-estimates of flow networks using inverse methods. Marine Ecology Progress Series. Oldendorf 42, 269–287.
Walters, C., Christensen, V., Pauly, D., 1997. Structuring dynamic models of exploited ecosystems from trophic mass-balance assessments. Reviews in Fish Biology and Fisheries 7, 139–172.